234P

Volume 84, number 5,6 OPTICS COMMUNICATIONS 1 August 1991

Full length article

A high power, high efficiency, laser-diode-pumped, continuous wave miniature Nd:glass laser

D.W. Hughes, J.R.M. Barr [1] and D.C. Hanna [1]

Department of Physics, University of Southampton, Southampton SO9 5NH, UK

Received 8 November 1990; revised manuscript received 7 February 1991

We report the operation of a Nd:glass laser pumped by a 500 mW broad single stripe laser diode. We have observed a slope efficiency of greater than 30% and an output power of greater than 100 mW when pumping with one diode. The output power increased to greater than 150 mW when two such diodes were used to pump the laser.

1. Introduction

The neodymium doped glass laser has been used for many years as a source of very short pulses, due its large fluorescence linewidth ($\Delta\nu = 5.3$ THz) (figure quoted for LG760 glass in ref. [1]). Actively mode locked systems have been developed using both flashlamp pumping and longitudinal pumping with argon ion lasers [2]. More recently the mode locked Nd:glass laser has been pumped using laser diodes [3], which show greater efficiency than argon lasers. There is currently much interest in the mode locking of solid state lasers using additive pulse mode locking (APM) [4]. In this technique, a portion of the laser output is directed into an external coupled cavity containing a nonlinear element. The pulse traversing the external cavity experiences an intensity dependent phase shift or amplitude change, and recombines interferometrically with the circulating pulse in the main laser cavity. This can result in the shortening of the pulse in the main laser cavity. This technique has been shown to be self-starting in several laser systems, e.g., Nd:YAG [5,6], Ti:Al_2O_3 [7], and Nd:YLF [8], with an intensity dependent threshold for the onset of the self-starting process (see, e.g., ref. [9]). The presence of this threshold indicates the need for the development of high output power, high slope efficiency laser-diode-pumped Nd:glass lasers if self-starting APM mode locking is to be achieved in this system. A high overall efficiency is mandatory in materials such as Nd:glass, where sensitivity to thermal effects is high. Self-starting APM has recently been reported for a krypton-laser-pumped Nd:glass laser [10]. An output power of approximately 250 mW was required for stable mode locking to be achieved.

In this paper we report the performance of a Nd:glass laser pumped by a single stripe 500 mW diode laser, yielding output powers of greater than 100 mW at a slope efficiency of approximately 30%. When this system was double-end pumped using two such diode lasers, output powers of greater than 150 mW were obtained.

Nd:glass lasers pumped by single stripe diode lasers have been reported previously [11,12], but due to the low power of the laser diodes used, the Nd:glass laser output was no greater than a few milliwatts. To significantly increase the output powers, laser diode arrays of typically ten or more elements have been used [3]. This in turn leads, however, to a reduction in the mode matching that can be achieved between the pump beam and the lowest order resonator mode, and hence to a lower slope efficiency and higher threshold. For example, Basu and Byer [12] have reported a threshold of 15.5 mW and a slope efficiency of 9.1% for pumping with a single stripe laser diode, using a very low transmission out-

[1] Also with the Opto-Electronics Research Centre, Southampton University.

put coupling (0.5%). Krausz et al. [3] have used a ten stripe laser diode array to pump a mode locked Nd:glass laser, reporting a threshold of 120 mW and a slope efficiency of 11%. However, in the latter case, a significantly higher output coupling was used (2.5%). For a cw system, using a ten stripe array as the pump source, we have previously obtained a threshold of 60 mW and a slope efficiency of 9.5%, using an output coupling of 1.5% [13].

2. Experimental arrangement

In our experiments, we have compared two 500 mW laser diodes, an SDL 2432 ten stripe laser diode array and an STC single stripe device. The relevant performance characteristics of these two lasers are shown in table 1. In each case the Nd:glass laser cavity was the same (fig. 1). The diode beam was focussed through the cavity rear mirror (>99.9% reflectivity at 1.05 μm, >90% transmission at 800 nm, ROC 2 cm) with a 3.2 cm focal length lens. The active medium was a 1.2 mm thick, 10 mm diameter disc of Schott LG-760 phosphate glass, with an 8% wt. Nd^{3+} concentration. This was placed at the focus of the cavity at Brewster's angle. The disc was held between two copper plates which had a clear aperture of 8 mm diameter. To compensate for the astigmatism produced by the active medium, a standard three mirror cavity was used [14]. The turning mirror was a 10 cm ROC mirror (>99.9% reflectivity at 1.05 μm), and the angle of incidence was 5.5°. A plane output coupler of reflectivity 98.5% was used. The total cavity length was 65 cm. The average spot size of the TEM_{00} mode in the active medium was calculated to be $(\overline{\omega_0^2})^{1/2} \approx 36$ μm, where the averaging has been performed taking into account the refractive index of the active medium.

The first diode laser pump used was the SDL 2432 ten stripe array. The diode beam was collimated using a 6.5 mm focal length lens, and passed through an anamorphic prism pair (×5 magnification) before being focussed into the Nd:glass resonator. The wavelength of the array was temperature tuned to coincide with the 800 nm absorption line using a Peltier cooler. By this means, greater than 90% of the incident diode radiation was absorbed in the glass. When the broad stripe laser diode (LQ-(P)-05) was used, the collimating and focussing arrangements were virtually the same, only the difference being that an anamorphic prism pair magnification of ×6 was used. This diode was mounted on a copper plate, and its wavelength temperature tuned using a Peltier cooler. The performance of the laser when the SDL laser diode array was used is shown in fig. 2. It can be seen from this figure that the slope efficiency decreases as the pump power is increased. This observation has lead us to consider the thermal effects which may be affecting the performance of this laser.

Table 1
Comparison of the main operating parameters of the two laser diodes used in this experiment.

	SDL 2432	STC LQ-P-05
Efficiency (mW/mA)	0.85	0.78
Emitting dimensions, μm	100×1 [a]	40×1
Beam divergence θ, deg		
parallel to junction	6.0	7.5
perpendicular to junction	28.5	25.0 [b]
Threshold current, mA	250	190
Operating current, mA	840	830
Room temperature wavelength, nm	812	805
Operating wavelength, nm	804	801

[a] The SDL 2432 is a 10 stripe array, each stripe is 3×1 μm.
[b] A two lobe structure was observed for the far-field pattern of the STC diode in the plane perpendicular to the junction.

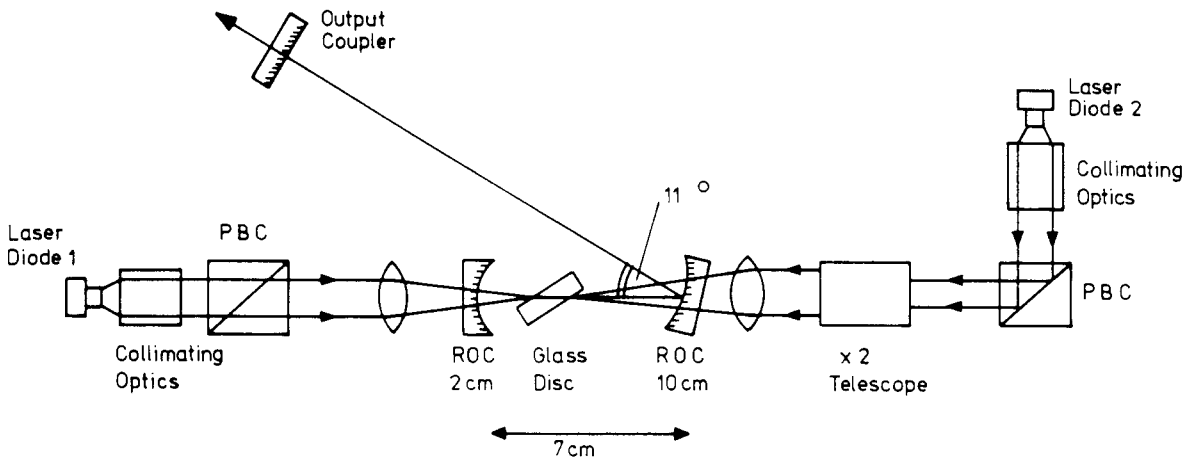

Fig. 1. Schematic diagram of the laser-diode-pumped Nd:glass laser. PBC: Polarizing beamsplitting cubes.

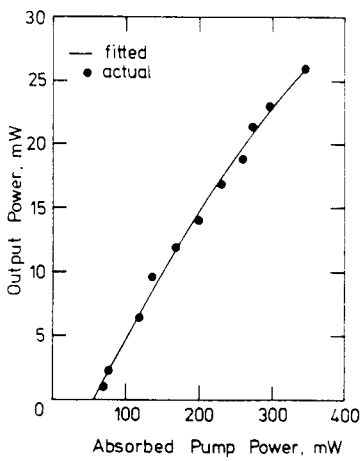

Fig. 2. Performance of the Nd:glass laser pumped by the SDL ten-stripe array.

3. Thermal effects

Thermal effects in solid state lasers are the result of the combined effect of the heat produced by absorption of the pump radiation together with heat flow due to the cooling processes (see, for example Koechner [15]). The effect of these two processes is to set up a temperature gradient in the active medium, which influences the optical behaviour of the laser beam in two main ways. Firstly, it gives rise to mechanical stresses in the rod, which will produce refractive index changes due to the photoelastic effect. This can produce birefringence effects in the active medium. Secondly, the variation of refractive index with temperature and with stress can give rise to a thermal focussing effect in the medium. We will consider each of these effects in turn.

3.1. Thermally induced birefringence

We have attempted to estimate the effect of thermally induced birefringence on the performance of the laser described in this work using the model of Koechner [15]. It should be noted that this model was developed for the case of uniform internal heat generation over an infinitely long rod. Although this model does not apply directly to our experiments, it is still useful to give an idea of the magnitude of the effects which may be expected.

The effect of thermally induced birefringence in the active medium will be to cause the partial depolarization of a linearly polarized beam passing through it. The thermally induced birefringence will thus lead to power being coupled into the orthogonal state of polarization. For a cavity containing a polarizing element (such as our cavity, where the glass was placed in the cavity at Brewster's angle) some of this power will then be removed from the cavity.

From Koechner, the depolarization loss of the resonator assuming a TEM_{00} mode is given by

$$L_{\mathrm{depol}} = 0.25(1 + 16/C_T^2 P_a^2)^{-1}. \qquad (1)$$

Volume 84, number 5,6 OPTICS COMMUNICATIONS 1 August 1991

The constants used in this paper are shown in table 2, and the variables in table 3. The values were obtained from ref. [1], and are quoted for LG-760 glass. For glass, which is isotropic, we obtain [15,16]

$$C_T = \frac{\alpha}{4\lambda_L K}\frac{E}{1-\nu}(B_1 - B_2)\,. \qquad (2)$$

C_T was thus calculated to be 0.718 W^{-1}.

From eq. (1) it can be seen that for the relatively low pump powers which we have used in our experiments, L_{depol} may be approximated by

$$L_{depol} = 0.25(C_T^2 P_a^2)/16) = BP_a^2\,. \qquad (3)$$

This relation gives the depolarization losses if the intra-cavity polarizer has a very high extinction ratio. In our case, where we essentially have a Brewster-surfaced polarizer in the cavity, the round-trip losses expressed by eq. (3) must be multiplied by a factor of 0.52 [15]. Using this factor, and inserting the value of 0.718 W^{-1} previously obtained for C_T, we obtain a value for the depolarization losses of $B = 4.2\times10^{-3}/W^2$, i.e. $4.2\times10^{-9}/mW^2$ of heat dissipated in the medium.

Table 2
Table of constants.

Symbol	Parameter	Value (where applicable)
λ_L	Emission wavelength	1.053 μm
λ_P	Pump wavelength	800 nm
n_0	Refractive index	1.508
dn/dT	Temperature coefficient of refractive index	$-6.8\times10^{-6}/°C$
B_1	Photoelastic constant	1.74×10^{-12} m^2/N
B_2	Photoelastic constant	3.73×10^{-12} m^2/N
P_{mn}	Elements of the photoelastic tensor	
E	Young's modulus	53.7×10^9 N/m^2
ν	Poisson's ratio	0.267
α	Coefficient of linear thermal expansion	$125\times10^{-7}/°C$
K	Thermal conductivity	0.6 W/m/K

Table 3
Table of variables.

Symbol	Parameter
P_o	Nd:glass laser output power
P_i	Total incident power absorbed
P_a	Total power dissipated as heat in the glass $P_a = (1-\lambda_P/\lambda_L)P_i = 0.23P_i$
$P_{th}(A+T+BP_i^2)$	Threshold pump power
η_s	Slope efficiency
Q	Heat generated per unit volume
L	Thickness of glass disc
r_0	Spot size of the pump beam ≈ 36 μm

3.2. Thermal lensing

To evaluate the possible effects of thermal lensing on the laser described in this paper, we have again used Koechner's model [15]. For the case of uniform heat generation in an infinitely long cylindrical rod, one obtains a parabolic radial temperature profile in the rod. The radial variation of the refractive index with temperature can then be shown to also be parabolic [15]. Taking into account the refractive index variation due to thermal strain, and end effects, the full expression for the rod focal length is given by [15,17]

$$f = \frac{\pi K r_0^2}{P_a}\left(\frac{1}{2}\frac{dn}{dT} + \alpha C_{r,\phi} n_0^3 + \frac{\alpha r_0 (n_0 - 1)}{L}\right)^{-1}\,. \qquad (4)$$

The first term in the brackets is due to the temperature dependence of the refractive index, the second term is due to its thermal stress dependence, and the third term is caused by end effects. C_r and C_ϕ are functions of the elements P_{mn} of the photoelastic tensor, and have been calculated as being 0.13 and 0.11 respectively. Insertion of the relevant parameters for our laser indicates that the end effects are small compared to the first two terms. Due to the fact that the stress dependent variation of refractive index is dependent on polarization of light, we obtain two values for the focal length of the thermal lens, f_r and f_ϕ. These refer respectively to the radial and tangential components of the polarized light, and have been calculated from eq. (4) as being +1.02 cm and +1.64 cm respectively for a pump power of 500 mW. It is interesting to note that these focal lengths each

Volume 84, number 5,6 OPTICS COMMUNICATIONS 1 August 1991

have a positive sign, despite the fact that dn/dT is negative. This arises from the fact that the magnitude of the thermal stress term is slightly larger than that due to the temperature dependent variation of the refractive index. The resonator will become unstable when the focal length of the thermal lens becomes approximately equal to one half of the confocal parameter of the cavity mode [18]. The confocal parameter has been calculated as being 7.7 mm. This indicates that the cavity will become unstable for pumping with a total power of approximately 1.3 W.

4. Experimental results and discussion

In this section, we present the performance of the laser-diode-pumped Nd:glass laser for pumping with the two different laser diodes, and we estimate the effect of thermally induced birefringence on the laser performance. This estimation was carried out by attempting to fit an expression of the form

$$P_o = \frac{kT}{A+T+BP_a^2}\left[P_i - P_{th}(A+T+BP_a^2)\right] \qquad (5)$$

to each of the slope efficiency curves presented. In eq. (5), P_o is the output power, P_i the absorbed pump power and $P_{th}(A+T+BP_a^2)$ the threshold pump power. The slope efficiency is given by

$$\eta_s = \frac{kT}{A+T+BP_a^2}, \qquad (6)$$

where k is a constant of proportionality. The term $A+T+BP_a^2$ in eq. (5) represents all the cavity losses. T is the output coupler transmission and A represents other non-power dependent cavity losses, such as leakage through the nominally highly reflecting mirrors. T was 1.5%, and A was measured to be approximately 0.3%. The BP_a^2 factor represents the power dependent cavity loss, which is ascribed to thermal birefringence. The quadratic dependence of this term was obtained from eq. (3).

Fig. 2 shows the performance of the Nd:glass laser when the SDL diode array was used as the pump source. The laser threshold was approximately 60 mW of absorbed pump power, and the slope efficiency for the initial part of the curve (absorbed pump power below 200 mW) was 11%. The value of B in this case was calculated from the fitting procedure to be $7.4 \pm 2.5 \times 10^{-7}/\mathrm{mW}^2$. It can be seen that this value of B is significantly larger than that calculated from the theory of Koechner [15]. It is believed that this is because, as stated previously, Koechner's model applies to a different situation than that which was prevalent in our experiments. It should be noted that for pumping with the SDL laser diode array, the Nd:glass laser could only be constrained to operate in the TEM_{00} mode by expanding the diode beam with a $\times 2$ telescope.

Fig. 3 shows the performance of the Nd:glass laser when the broad stripe diode (STC LQ-(P)-05) was used as the pump source. Initially the same pumping configuration was used, with the telescope present. The laser threshold and slope efficiency were, respectively, 45 mW and 12.5%. This improved performance is attributed to slightly better mode matching between the Nd:glass resonator lowest order mode and the pump beam. The value of B obtained from the fitting procedure was $8.5 \pm 1.2 \times 10^{-7}/\mathrm{mW}^2$.

Using the STC broad stripe diode, single transverse mode operation of the Nd:glass laser could also be obtained without using the telescope. The performance of the laser using this pump geometry is shown in fig. 4. The pump threshold is 48 mW, and the slope efficiency for pump powers below 200 mW is 32%. This three-fold increase in the slope effi-

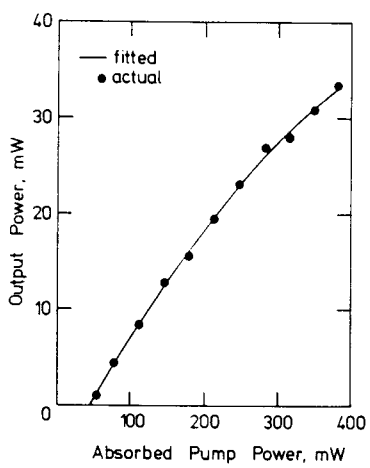

Fig. 3. Performance of the Nd:glass laser pumped by the STC laser diode, with the same collimating/focussing arrangement as for fig. 2.

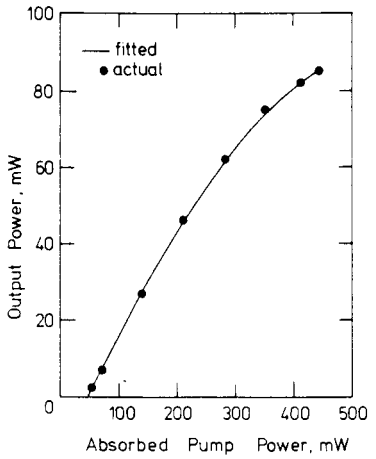

Fig. 4. Performance of the Nd:glass laser pumped by the STC laser diode with the expanding telescope removed.

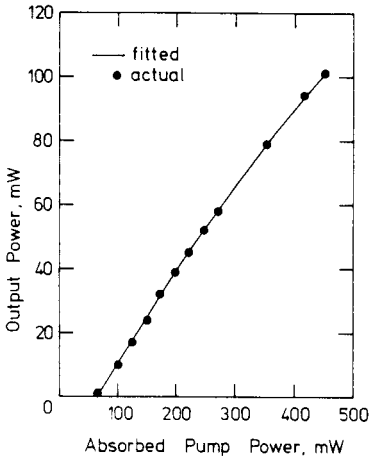

Fig. 5. Performance of the Nd:glass laser pumped by the STC laser diode with improved heat sinking of the glass disc.

ciency is attributed to the increased brightness of the pump beam, leading to a better overlap of the pump beam and the laser resonator mode. The curve fitting analysis yields a value for B of $9.0\pm0.3\times10^{-7}/\mathrm{mW}^2$, in good agreement with the previous case.

The effects of thermally induced birefringence have been significantly reduced by improved heat sinking of the glass disc. To achieve this, the copper plates holding the disc were replaced by plates (also copper) with a smaller clear aperture. This ensures that a much greater proportion (91% as opposed to 36%) of the glass faces is in contact with the holders. In addition, to ensure good thermal contact between the glass and the copper plates, a thin (100 μm) layer of indium was placed between each of the glass plates and the copper plates (100 μm thick copper foil has also been used, and gave similar results).

The improved performance of the laser with this set-up is shown in fig. 5. The reduction in slope efficiency with increasing pump power is less marked, due to a decrease in the value of the "birefringence constant" B to $2.6\pm0.3\times10^{-7}/\mathrm{mW}^2$. The pump threshold and slope efficiency were 63 mW and 30% respectively, where the slope efficiency has again been quoted for the initial part of the curve. We have attempted to increase the power from this laser by pumping with two polarization coupled STC laser diodes. We have observed, however, that the output power in this case is restricted by the surface of the glass disc being melted at a combined pump power of approximately 600 mW.

In an attempt to overcome this thermal damage problem, we pumped the glass disc with two STC LQ-(P)-05 laser diodes from opposite ends of the laser cavity i.e. the second diode (diode 2) pumped the disc through the 10 cm ROC turning mirror as shown in fig. 1. This geometry ensured a more uniform temperature distribution in the disc. The collimating optics used were the same as for the other diode (diode 1), but a lens of 7.5 cm focal length was used to focus the diode beam through the turning mirror. It was also necessary to use a $\times2$ telescope before focussing to achieve TEM_{00} operation of the Nd:glass laser when pumped by diode 2 alone. The diodes were isolated from each other using two polarizating beam-splitting cubes. To achieve the correct polarization for reflection from the relevant cube, diode 2 was mounted orthogonally to diode 1. The performance of the glass laser when pumped by diode 2 alone is shown in fig. 6. The relatively low maximum pump power incident on the glass disc (350 mW) was due to the pump beam being apertured on the focussing lens holder and the turning mirror holder. Also, the pump power absorbed in the glass disc is reduced by approximately 15% due to Fresnel reflection at the input surface of the glass. The performance of the glass laser when pumped by both diodes simultaneously is shown in fig. 7. The system was set up to give maximum output power (153 mW) with both

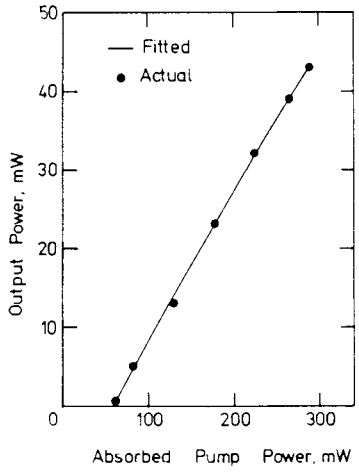

Fig. 6. Performance of the Nd:glass laser when pumped by diode 2 alone.

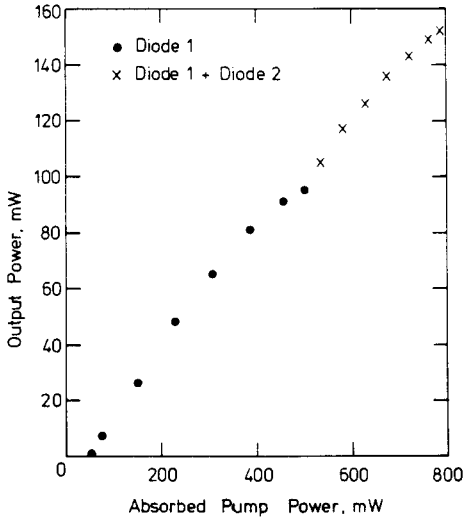

Fig. 7. Performance of the Nd:glass laser when pumped by diodes 1 and 2 simultaneously.

diodes pumping simultaneously. It should be possible to further increase the power output beyond 153 mW by a more careful choice of focussing lens holder, and by using a larger diameter turning mirror. For a pump power of 500 mW from diode 2, we believe we should be able to obtain greater than 180 mW from the Nd:glass laser.

We have investigated the polarization properties of the glass laser output. A polarizing beam splitter

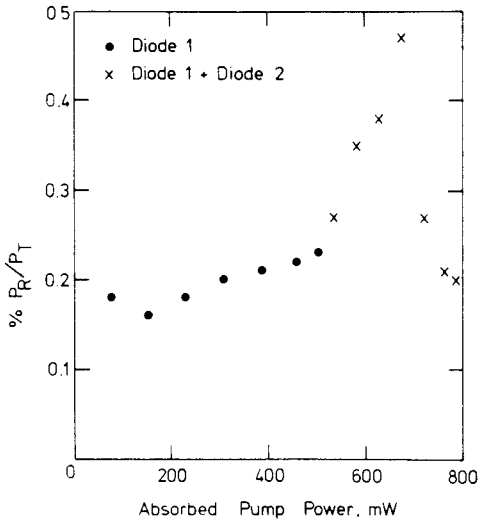

Fig. 8. Variation of the ratio P_R/P_T with absorbed pump power.

was placed in the output beam, and the transmitted and reflected powers (P_T and P_R respectively) were monitored as the diode laser outputs were varied. A plot of the variation of the ratio P_R/P_T is shown in fig. 8. Although the precise shape of this curve was highly dependent on the exact position of the focussed beams in the glass, a similar trend was always observed. As the power from diode 1 was increased, the ratio increased, as one would expect due to increased thermal birefringence in the glass. When diode 2 is turned on and its output increased, the ratio increased at a faster rate, and then decreased. We have thus observed the somewhat surprising result that as the absorbed pump power was increased, the internal cavity losses appeared to decrease. We believe that this partial "birefringence compensation" may be due to the fact that the glass was being pumped by, essentially, two elliptical beams whose major axes were mutually orthogonal. The thermally induced birefringence due to one of these beams can then be considered to reduce and possibly cancel that caused by the other. This effect is currently under further investigation.

5. Conclusions

We have demonstrated the operation of a high power, high slope efficiency (>30%) laser-diode-

pumped Nd:glass laser. We believe that the maximum output power we have obtained from this laser 153 mW, could be increased still further by improvement of the pump geometry for laser diode 2. These results are a significant improvement on those reported previously for laser-diode-pumped Nd:glass lasers. We have also observed an interesting property of this system, whereby the combined effect of pumping with two mutually orthogonal pump beams simultaneously appears to cause a decrease in the amount of thermally induced birefringence.

Acknowledgement

The authors are grateful to David Daniel of STC Optical Devices (Paignton, U.K.) for supplying several 500 mW broad stripe laser diodes. This work was supported by the Science and Engineering Research Council (SERC). D.W.H. gratefully acknowledges financial support from SERC. We are also grateful to the referee for his comments concerning the efficiency of the Nd:glass laser when pumped by diode 2.

References

[1] Schott laser glass handbook.
[2] L. Yan, P-T. Ho, C.H. Lee and G.L. Burdge, IEEE J. Quantum Electron. QE-25 (1989) 2431.
[3] F. Krausz, T. Brabec, E. Wintner and A.J. Schmidt, Appl. Phys. Lett. 55 (1989) 2386.
[4] J. Mark, L.Y. Liu, K.L. Hall, H.A. Haus and E.P. Ippen, Optics Lett. 14 (1989) 48.
[5] L.Y. Liu, J.M. Huxley, E.P. Ippen and H.A. Haus, Optics Lett. 15 (1990) 553.
[6] J.R.M. Barr and D.W. Hughes, Appl. Phys. B 49 (1989) 323.
[7] J. Goodberlet, J. Wang, J.G. Fujimoto and P.A. Schulz, Optics Lett. 14 (1989) 1125.
[8] J. Goodberlet, J. Jacobson, J.G. Fujimoto, P.A. Schulz and T.Y. Fan, Conf. on Lasers and electro-optics (CLEO, Anaheim, May 21–25, 1990), paper TuB6PD.
[9] J. Goodberlet, J. Jacobson, J.G. Fujimoto, P.A. Schulz and T.Y. Fan, Optics Lett. 15 (1990) 504.
[10] F. Krausz, Ch. Spielmann, T. Brabec, E. Wintner and A.J. Schmidt, Optics Lett. 15 (1990) 1082.
[11] W. Kozlovsky, T.Y. Fan and R.L. Byer, Optics Lett. 11 (1986) 788.
[12] S. Basu and R.L. Byer, Optics Lett. 13 (1988) 458.
[13] D.W. Hughes, J.R.M. Barr and D.C. Hanna, Optics Lett. 16 (1991) 147.
[14] H.W. Kogelnik, E.P. Ippen, A. Dienes and C.V. Shank, IEEE J. Quantum Electron. QE-8 (1972) 373.
[15] W. Koechner, Solid-state laser engineering (Springer, Berlin, 1988) ch. 7.
[16] J.M. Eggleston, T.J. Kane, K. Kuhn, J. Unternahrer and R.L. Byer, IEEE J. Quantum Electron. QE-20 (1984) 289.
[17] H.W. Kogelnik, Bell Syst. Tech. J. 44 (1965) 455.
[18] F. Krausz, E. Wintner, A.J. Schmidt and A. Dienes, IEEE J. Quantum Electron. QE-26 (1990) 158.